

MULTIVARIATE APPROACH OF END-MEMBER CONTRIBUTIONS TO
STREAMFLOW IN THE CRITICAL ZONE. CASE STUDY: VALLES CALDERA,
NEW MEXICO

by

Rodrigo Andrés Sánchez

Copyright © Rodrigo Andrés Sánchez 2019

A Thesis Submitted to the Faculty of the

DEPARTMENT OF HYDROLOGY AND ATMOSPHERIC SCIENCES

In Partial Fulfillment of the Requirements

For the Degree of

MASTER OF SCIENCE

WITH A MAJOR IN HYDROLOGY

In the Graduate College

THE UNIVERSITY OF ARIZONA

2019

THE UNIVERSITY OF ARIZONA
GRADUATE COLLEGE

As members of the Master's Committee, we certify that we have read the thesis prepared by Rodrigo Andres Sanchez Romero, titled Multivariate Approach of End-Member Contributions to Streamflow in the Critical Zone. Case Study: Valles Caldera, New Mexico and recommend that it be accepted as fulfilling the dissertation requirement for the Master's Degree.

Thomas Meixner

Thomas Meixner (Jan 10, 2020)

Thomas Meixner, Ph.D.

Date: Jan 10, 2020

Jennifer C McIntosh

Jennifer C McIntosh (Jan 10, 2020)

Jennifer McIntosh, Ph.D.

Date: Jan 10, 2020

Jon Chorover

Jon Chorover, Ph.D.

Date: Jan 14, 2020

Final approval and acceptance of this thesis is contingent upon the candidate's submission of the final copies of the thesis to the Graduate College.

I hereby certify that I have read this thesis prepared under my direction and recommend that it be accepted as fulfilling the Master's requirement.

Thomas Meixner

Thomas Meixner (Jan 10, 2020)

Thomas Meixner, Ph.D.

Master's Thesis Committee Chair

Hydrologic and Atmospheric Sciences

Date: Jan 10, 2020

ARIZONA

ACKNOWLEDGEMENTS

This study was supported by the National Science Foundation funded Jemez River Basin and Santa Catalina Mountains Critical Zone Observatory. I would like to thank my thesis advisor Dr. Thomas Meixner and my committee members Dr. Jennifer McIntosh and Dr. Jon Chorover for their guidance. I would also like to thank the CZO collaborators that have made the data available for this investigation; special thanks to Alissa White, Mark Losleben, Xavier Zapata-Rios and Kate Condon for all the fieldwork and sample collection.

TABLE OF CONTENTS

LIST OF FIGURES	5
LIST OF TABLES	6
ABSTRACT.....	7
1. INTRODUCTION.....	8
2. STUDY AREA.....	11
2.1 Geology	12
2.2 Hydrology.....	12
3. METHODS.....	15
3.1 End-members and surface water samples.....	15
3.2 Principal component analysis and end-member mixing analysis	17
4. RESULTS.....	20
4.1 Conservative tracers and Principal Component Analysis.....	20
4.2 End-members selection and projections	22
5. DISCUSSIONS	24
5.1 Analysis of U-mixing spaces.....	24
5.2 End-members contributions and streamflow generation: Hydrologic responses	27
6. CONCLUSIONS	34
7. FIGURES AND TABLES.....	35
8. REFERENCES	47

LIST OF FIGURES

Figure 1. Location of the Valles Caldera National Preserve in northern New Mexico. Redondo Peak, headwater catchments draining different aspects and springs locations around the dome.....	35
Figure 2. Conservative tracers evaluated by plotting medians of potential end-members along with solute concentrations of stream flow. (a) Shows an example of a bivariate plot with two tracers that are used in PCA, whereas (b) presents two tracers that cannot be utilized in PCA. A total of 55 mixing diagrams were evaluated for each catchment.	36
Figure 3. Orthogonal projection of end-members, onto (a) 2-D and (b) 3-D mixing U-spaces defined by stream water chemistry in La Jara catchment.....	37
Figure 4. Orthogonal projection of end-members, onto (a) 2-D and (b) 3-D <i>U</i> spaces defined by stream water chemistry in Upper Jaramillo catchment.	38
Figure 5. Orthogonal projection of end-members, onto (a) 2-D and (b) 3-D <i>U</i> spaces defined by stream water chemistry in History Grove catchment.....	39
Figure 6. Calculated fractional contribution of selected end-members of the (a) La Jara, (b) Upper Jaramillo, and (c) History Grove creeks.....	40
Figure 7. Factor Analysis of principal components retained for each mixing space.....	41

LIST OF TABLES

Table 1. Chemical composition of potential end-members	433
Table 2. Cumulative percentage of the eigenvalues from each eigenvector for each catchment.	45
Table 3. Calculated Euclidean distances expressed in percentages for each conservative tracer	46

ABSTRACT

Multivariable End-member Mixing Analysis (EMMA) that incorporates principal component analysis (PCA) is a widely utilized tool to identify the sources of water that generate streamflow in catchment hydrology. In this study we investigated how different combinations of principal components (PC) allow assessing the importance that potential end-members have to surface waters. We evaluated mixing spaces of different dimensions in order to justify the number of end-members needed to generate streamflow. Furthermore, this multidimensional approach provided further evidence of the hydrologic processes that dominate in the headwaters at the Jemez River Basin Critical Zone Observatory (JRB-CZO).

Our results showed that the U-mixing spaces of three dimensions of the La Jara and Upper Jaramillo catchments highlight the contributions of deep ground water that the two-dimensional mixing space neglected. Conversely, in the History Grove catchment a two-dimensional U-mixing space was enough to explain stream flow generation.

Groundwater, snowmelt, rainfall and soil water are the end-members identified in each catchment. The geomorphology (e.g. aspect, topography and geology) of each watershed and climate variability, however, influence the contribution of these source waters in each system. Groundwater contributions dominate streamflow generation in the JRB-CZO.

Moreover, increments of snowmelt, rainfall and soil water contributions are observed specifically during base flow conditions. We argue that the contributions of these end-members do not correspond specifically to overland flow, but rather contributions of shallow groundwater and subsurface lateral flow that possess the chemical signature of these source waters.

1. INTRODUCTION

Climate change has affected the amount and spatial distribution of precipitation (i.e. rainfall and snowfall) worldwide. Changes in intensity and spatial variability of these precipitation inputs have negative implications in catchment hydrology affecting water partitioning processes and streamflow generation (Fee et al., 1996). Watersheds located in the Southwestern United States are particularly sensitive to these changes. This region's bimodal precipitation pattern, i.e., snowfall during the winter and rainfall during the summer monsoons, is responsible for most of the water inputs of these semi-arid systems. Shifts in these precipitation patterns can negatively affect how water is distributed within a watershed, which makes these ecosystems particularly vulnerable to climate variability and drought (Molotch et al., 2009).

Terrain aspect controls the amount of energy and effective precipitation inputs within a catchment. These differences influence the catchment's geological, physical, chemical, and biological processes (Lyon et al., 2008; Broxton et al., 2009; and Zapata et al., 2015). Moreover, vegetation cover and hydrologic processes such as accumulation, sublimation and melting of snow, evapotranspiration, soil moisture, and shallow and deep subsurface flow are aspect mediated (Zapata et al. 2015b; Hinckle et al., 2012). The amount of time that water takes to reach the outlet of the catchment—water transient time (WTT)—varies depending upon the path it takes (McGuire et al., 2005)), i.e. water can quickly flow through the surface and/or the immediate subsurface, or even percolate into the deep subsurface reaching the groundwater. Furthermore, as water moves through the vadose zone and groundwater reservoirs, mineral dissolution and other chemical processes occur, thereby varying its chemical signature. These changes in solute

concentrations depends upon, but is not limited to, the surrounding geology, e.g. soil, regolith, fractured bedrock, as well as climate conditions and vegetation type (Rademacher et al, 2005). Ultimately, these chemically distinct waters converge into the surface water influencing its chemistry.

Streamflow generation is driven by the mixing of multiple source waters (i.e. end-members). This process can occur either as direct input, i.e. snowfall and rainfall, or by water that has been transported and biogeochemically transformed through the soil, regolith, and bedrock (groundwater) (Christophersen and Hopper, 1992). The differences of solute concentrations of the potential end-members, e.g. very dilute for rainfall and snowfall versus more concentrated for soil water and groundwater, have been the starting point of various studies that have sought to identify and quantify the contributions of source waters to streamflow (Lui et al., 2004; Doctor et al., 2006; Lui et al., 2008a; Liu et al., 2008b). These studies have successfully applied the end-member mixing analysis (EMMA) approach to quantify the percentage contribution of end-members to generate streamflow in watersheds. EMMA is a tracer-based methodology that assumes conservative mixing—non-reactive mixing—of multiple source waters. The simplest approach is to utilize two tracers, e.g. silicon and chloride, to create a two-dimensional space that allows identifying a maximum of three end-members. Moreover, depending on the catchment's physical and geochemical processes, various source waters may feed the surface waters, e.g. overland flow, lateral subsurface flow, shallow and deep groundwater, thus multiple tracers may be required to assess the interaction of these source waters with streamflow. In a multi-tracer approach the chemical constituents are not independent from one another but rather have a degree of correlation. Principal

component analysis (PCA) has been extensively utilized in mixing models when multiple tracers are considered in the analysis (Christophersen and Hooper, 1992)—PCA creates a new mixing space that is dimensionally smaller than the original. This subspace, also known as U-space, comprises those principal components (PC) that are orthogonal to each other and that explain most of the variability of the original data (Liu et al., 2008a).

The existing literature reports several studies that have combined PCA and EMMA to evaluate contributions of end-members to streamflow (Christophersen and Hooper, 1992; Hooper et al., 2003; Liu et al., 2008a; Liu et al., 2008b, Correa et al., 2017 Dwivedi et al., 2019). These case studies have shown coherent results when analyzing U-spaces of two dimensions, i.e. retaining two principal components, identifying up to three end-members. Nevertheless, hydrological and geological setting of catchments, as well as limited access, identification and characterization of potential source waters, have deterred further interpretation of how these results may vary when assessing more than one combination of PCs, i.e. mixing U-spaces of multiple dimensions.

This study aims to assess how changing the number of principal components retained in an EMMA analysis can strengthen the justification of potential end-members that generate streamflow. Furthermore, we conceptualize how terrain aspect, subsurface structure, and climate variability influence preferential water flow paths within montane catchments in the sub-humid western United States.

2. STUDY AREA

The critical zone (CZ) is the near-surface environment that extends from the top of the canopy through the saturated zone to unweathered bedrock, where the majority of the earth's life occurs (Brantley et al. 2007, Chorover et al., 2011). The CZ is a dynamic and variable system driven by mass and energy fluxes, where the bedrock, soil, water and life interact biologically, chemically and physically (Chorover et al., 2011).

This study takes place in Jemez River Basin Critical Zone Observatory (JRB-CZO) located in the Valles Caldera National Preserve (VCNP) in northern New Mexico (Figure 1). The approximately 20 km diameter caldera was the result of the most recent eruption of the Jemez volcanic field when the magma chamber underneath collapsed about 1.25 Ma (Chipera et al., 2008; Woff et al., 2011). Following the caldera-forming event the deposition of laminated and bedded sediments, sporadic eruptions of rhyolite lava and tuff, and uplift and deformation of the land surface define the geology and geomorphology of the Valles Caldera (Chipera et al., 2008). The highest point in the VC, Redondo Peak dome at 3435 m.a.s.l, rises from the center of the valley and hosts several first-order streams (headwaters) that drain towards the East Fork Jemez River, which is a tributary of the Rio Grande River (Lyon et al., 2008; Zapata et al., 2015).

The annual average precipitation in the valley is approximately 476 mm. Approximately half of this precipitation falls as snow during the winter (October to April), and the remaining fraction occurs as rainfall during the summer monsoons (July and August) (Liu et al., 2008a; Porter, 2012). The climate at the Valles Caldera is classified as montane, but it is also often referred to as semiarid due to its location between the snow dominated Rocky Mountains and the southwestern United States

deserts. High vapor pressure deficits during the summer make this site particularly sensitive to droughts and climate change (Broxton et al. 2009). The average temperature at the VC is about 9 °C, going up to 25 °C in the summer and down to -15 °C in the winter (Lyon et al., 2008; Broxton et al., 2009).

2.1 Geology

Redondo Peak dome is composed of Pleistocene deposits principally composed of dense rhyolite ash-flow tuff (Goff et al., 2006). The major minerals found among the bedrock of Redondo Peak are quartz, plagioclase feldspar (albite and oligoclase), alkali feldspar (sanidine), and small amounts of smectite and zeolite (Vasquez-Ortega, 2015). Even though rock types are well defined around the dome, its soil composition presents a more complex structure. Weathering of feldspar, volcanic glass and primary minerals into kaolinite and smectite is the predominant process of soil genesis. However, due to physical erosion, ash, and modern dust deposition, soil profiles around Redondo Peak show clear discontinuities (Rasmussen et al., 2012). Soils within the study area are classified as well drained Mollisols, Inceptisols and Alfisols ranging from coarse sandy loam to clay loam textures with the presence of partial to high decomposed organic matter in surface soil horizons (Vasquez-Ortega, 2015; Zapata et al., 2015).

2.2 Hydrology

The East Fork Jemez River (EFJR) crosses the Valle Grande in the VCNP. Its drainage area is approximately 120 km², and it drains south-west joining San Antonio Creek to form the Jemez River (Liu et al., 2008b). Near-surface runoff, shallow subsurface flow and groundwater are likely to be the most relevant source waters to the EFJR as determined by EMMA (Liu et al., 2008b). These end-member contributions vary

seasonally, being the snowmelt and monsoon seasons responsible for high contributions of near-surface runoff. Shallow subsurface flow becomes more relevant as snowmelt progresses and the monsoon begins, whereas the mean calculated groundwater contribution fluctuates between 20% and 40%, and it has been hypothesized that the deep groundwater and surface waters are both hydrologically and geochemically connected (White et al., 2019), and that during relatively wet winters deep groundwater flushes into streams increasing discharge (Q) (Liu et al., 2008b, McIntosh et al., 2017).

On the west side of the EFJR, three streams flow from the terrain around Redondo Peak. Lateral subsurface flow and groundwater dominate surface water flows (Liu et al., 2008a). The La Jara, Upper Jaramillo and History Grove catchments (Figure 1) are the focus of this study. Base cations concentrations and dissolve organic carbon (DIC) strongly correlate with water transient times (WTT), suggesting that primary minerals weathering reactions control the fluxes of these solutes (Zapata-Rios et al., 2015). Moreover, the chemostatic behavior of base cation concentrations in surface water suggests that groundwater is likely the dominant water supply in the three catchments (Zapata-Rios et al., 2015; Lyon et al. 2008; White et al., 2019). Furthermore, terrain aspect mediates the hydrologic responses among the three catchments around the dome. Fluxes of energy and mass control water availability in the system, leading to differences in groundwater recharge, snowmelt, sublimation, and evapotranspiration among these headwaters (Zapata-Rios et al., 2016).

Major cation and anion concentrations in the surface water around Redondo Peak suggest that the export of these solutes is primarily dominated by the weathering of Ca-rich (anorthite) and Na-rich (albite) plagioclase feldspar. Though it is unlikely that calcite

is present in areas where volcanic material prevails, Ca/Sr ratios in the La Jara creek indicate that the weathering of disseminated calcite found in the soil and bedrock contributes to stream Ca^{2+} concentrations (Porter, 2012; White et al., 2019). Furthermore, small variability in Ca^{2+} and DIC concentrations in surface waters suggests that soil water is thought to be an important contributor to streamflow during snowmelt seasons (Olshansky et al., 2018). Moreover, europium anomalies observed in soil and stream waters support the hypothesis that the weathering of plagioclase controls the solute composition in the streams along with the influence of dust deposition (Vázquez-Ortega et al., 2015).

3. METHODS

Semi-arid river systems, such as the JRB-CZO, rely on groundwater reservoirs, e.g. deep or shallow aquifers, to generate streamflow (McIntosh et al., 2017; Zapata et al., 2015; Liu et al., 2008a). Nonetheless, water moving on the near surface and shallow subsurface, i.e. lateral subsurface flow, may be important during periods of high discharge, e.g. snowmelt and monsoon seasons (Liu et al., 2008a). Furthermore, catchment physical properties, e.g. aspect and geology, may influence water paths in the subsurface before reaching streams (Zapata et al., 2016).

A multivariate end-member mixing analysis based on principal component analysis has proven to be an effective approach that allows accurate identification and quantification of end-member contributions (Christophersen and Hooper, 1992; Hooper et al., 2003). This study follows the methodology presented in the aforementioned studies, although we focus on the dimensionality of the mixing spaces (U-space). More specifically, we aim to justify the number of potential end-members that feed the surface water in each catchment by assessing mixing spaces of different dimensions.

3.1 End-members and surface water samples

Water from the streams and potential end-members, e.g. snow, rain, soil water and groundwater, were sampled and analyzed for major cation and anion concentrations, and water isotopes. In each flume installed at the outlet of each catchment (Figure 1), discharge is periodically estimated based on water height measurements given by pressure transducers, and standard stage-discharge relationships of each flume. Water samples for major cation analysis were collected in acid-washed 250 ml high density polyethylene (HDPE) bottles, and 500 mL DI-washed and combusted (475 °C, 4h) were

used to collect samples for dissolved inorganic carbon (DIC) and anions analysis. Surface water samples were collected weekly from the flume of each creek during the snowmelt and monsoon seasons from water years 2011 and 2012, and monthly during dry periods, i.e. pre-snowmelt and summer. Nine perennial springs around the dome have been identified and sampled monthly in each water year except during the winter months due to inaccessibility issues (Zapata et al., 2015). For the purpose of this study, we used these springs as proxies of groundwater and we treated them as individual sources. Six instrumented pedon sites installed within a zero order basin (ZOB) at the top of the La Jara catchment (Figure 1), collect soil water samples from Prenart lysimeters at multiple depths (3 cm to 115 cm). These samplers have been installed following the procedures in Lohse and Matson (2005). These soil water samples were divided in two subsets, i.e., deep and shallow soil waters end-members.

Snow samples were collected from snow pits, stored in one-gallon Ziploc bags and maintained frozen until complete melting at room temperature prior to filtering (Gustafson et al. 2010). Rainwater samples were collected in DI-washed 500 ml HDPE bottles from bulk rain collectors at two sites (Figure 1). A 500 mL bottle that contained a thin layer of mineral oil was used to collect samples for water isotopes analysis in order to prevent isotopic values changes due to evaporation (Zapata et al.,2015). All the water samples were properly packed, kept at 4 °C and transported to The University of Arizona laboratory facilities for subsequent analysis.

Prior to the analysis, all samples were filtered with a 0.45 µm nylon filter. Major cations were analyzed utilizing an inductively coupled plasma mass spectrometer (ICP-208 MS) (ELAN DRC-II, Perkin Elmer, Shelton CT) at the University of Arizona

Laboratory for Emerging Contaminants (ALEC). DIC samples were run with a Shimadzu TOC-VCSH 210 Carbon analyzer in ALEC. Water isotopes ($\delta^{18}\text{O}$ and δD) were measured with a DLT-100 Laser Spectrometer for liquid water stable isotopes with a reported instrument precision of ± 0.12 ‰ VSMOW at the University of Arizona.

It is important to point out that this chemistry data set is not consistent for all the solute concentrations. There exist missing data points which mean that the sample has not been analyzed for certain solutes primarily because sample volume did not meet volume necessary for the laboratory procedure. Additionally, we excluded samples that showed very dilute concentrations for some solutes that were not detected by the instrument. This data screening reduced the number of samples available for the analysis and may affect interpretation of the results.

3.2 Principal component analysis and end-member mixing analysis

The mixing model developed in this study followed the methodology proposed by Christophersen and Hooper (1992). Mixing models that are built upon a multidimensional solute matrix, i.e. multiple solutes can be considered tracers, often rely on PCA to reduce the dimension of the original data set without losing detail or any underlying patterns originally observed (Page et al., 2012). Thus, the number of potential end-members that contribute to generate streamflow in each catchment was determined based on the cumulative variance that is explained by the eigen vectors, i.e., principal components (PC), extracted from PCA. Moreover, Hooper (2003) provides further guidance for determining the number of conservative tracers and the selection of end-members in each catchment.

Conservative tracers were evaluated following the methodology of Liu et al. (2004). Conservative tracers were determined using mixing diagrams where stream samples were plotted along with the median of potential end-members, choosing those analytes that best bound the end-members and the streamflow samples.

The chemistry data of the three headwaters was normalized—this reduces the calculations to be biased towards extreme values. The stream water samples were standardized by subtracting the mean (\bar{x}_j) and divided by the standard deviation (s_j) of the concentration of each solute for each observation. The subscripts i and j represent each observation and solute respectively. The standardized values (x_{ij}^*) are calculated as follows:

$$x_{ij}^* = \frac{(x_{ij} - \bar{x}_j)}{s_j} \quad [1]$$

Concentrations of potential end-members were normalized relative to the stream water samples. The median of the solute concentrations of the selected end-members and the mean and standard deviation of the streams were used in equation [1].

Principal component analysis (PCA) was then applied to the normalized data. This analysis was conducted using JMP®, Version 11.0 (statistical software). The method of analysis selected in JMP® was REML (restricted maximum likelihood) which is useful for small datasets, as it uses all the data available, even if missing values are present. The eigen values and eigen vectors that explained most of the variance of the data set were extracted in each catchment.

Orthogonal projection of the streamflow into the new space—U matrix ($m \times n$)—was determined by equation [2]:

$$U = X^*V^T \quad [2]$$

where X^* is normalized matrix of stream flow chemistry ($n \times p$), n is the number of observations, and p the number of solutes included in the PCA. V represents the eigenvectors matrix ($m \times p$) where m represents the number of eigenvectors that explain most of the variance of the original chemistry data.

The projected streamflow chemistry matrix (\hat{X}^*) is calculated using equation [3].

$$\hat{X}^* = X^*V^T(VV^T)^{-1}V \quad [3]$$

\hat{X}^* can be destandardized to get a new chemical space (\hat{X}) by multiplying by the standard deviation of each solute and adding the correspond mean. Euclidian distances (d_j), also known as residuals, between the original chemistry and projections were calculated for each solute by the following equation:

$$d_j = \|\hat{b}_j - b_j\| \quad [4]$$

where subscript j represents each solute, b_j and \hat{b}_j are the original and projected solute values respectively. A similar procedure was followed to project the potential end-member into the U-spaces of each catchment.

Finally, Potential end-members in each catchment were identified in the U-mixing diagrams (Figures 3, 4 and 5). The end-members that best enclose all or most of the stream water samples were selected potential source waters. The number of end-members in each catchment is the number of eigenvectors—the number of principal components that define the U-mixing space—plus one ($m+1$). Additionally, Euclidean distances can be used to validate the end-member choice—the smaller the distance, the better the projection of end-embers onto the U-spaces are.

4. RESULTS

4.1 Conservative tracers and Principal Component Analysis

The solute concentrations used in this study were taken from the Jemez-River Basin Critical Zone Observatory geochemistry data set. Sample frequency availability for major cation and anion concentrations of each catchment were assessed in order to determine which solutes to include in the analysis. The selected solutes were: total inorganic carbon (TIC), total organic carbon (TOC), sulfate (SO_4^{2-}), chloride (Cl^-), sodium (Na^+), potassium (K^+), magnesium (Mg^{2+}), calcium (Ca^{2+}), silica (Si^{4+}), and stable water isotopes, i.e. $\delta^{18}\text{O}$ and δD . Moreover, one of the main assumptions of an EMMA analysis is conservative mixing, i.e. non-reactive, thus prior to further analysis it is imperative to determine which of these chemical constituents can be considered conservative. To this end, conservative tracers were evaluated following the methodology of Liu et al. (2004). Mixing diagrams of paired solute concentrations of surface water samples of each catchment (La Jara, Upper Jaramillo and History Grove) were plotted along with the median of potential end-members, e.g. snowmelt, rainfall, deep and shallow soil waters, and groundwater. A total of 55 plots of all possible combinations of coupled tracers were analyzed for each catchment. From these diagrams a pair of solutes were considered acceptable if most of the surface water samples were enclosed by three or more potential end-members (Figure 2). Thus, for the La Jara catchment seven tracers were found to be conservative: TIC, Cl^- , K^+ , Ca^{2+} , Si^{4+} , $\delta^{18}\text{O}$ and δD ; whereas TIC, K^+ , Mg^{2+} , Si^{4+} , $\delta^{18}\text{O}$ and δD , seemed to be conservative for the Upper Jaramillo and History Grove catchments.

Subsequently, once PCA was performed for each solute matrix of each catchment, the number of principal components was determined based on the variability explained by each data set. There is no exact solution to this problem, but the simplest approach is to consider the cumulative percentage variance contribution obtained for successive eigenvalues until it is considered sufficiently high, e.g. 80% or higher. This value varies depending on the nature of the data, e.g. the degree of collinearity and redundancy in it (Reyment and Jvreskog, 1996). Furthermore, Hooper (2003) argues that the eigenvalues and eigenvectors, i.e. principal components (PC), extracted from PCA do not explain all the variance of the original data set, but rather part of this variance could be considered as noise. Thus, the "rule of 1" establishes that the retained eigenvectors, or PC, should explain at least $1/(\text{number of tracers})$ of the stream chemistry variance (Hooper, 2003), e.g. if eight solutes comprised the solute matrix for PCA, at least one-eighth (12.5%) of the variation of the data should be explained by each eigenvector to be retained. Therefore, the minimum variance that is expected to be explained by the eigenvectors for the La Jara catchment is 14.29% (one-seventh), and 16.67% (one-sixth) for the Upper Jaramillo and History Grove catchments (Table 2).

Using this rule and based on the PCA results (Table 2), the first two PC fulfill the "rule of 1" explaining 80.36% and 75.18% of the water chemistry variance for the La Jara and Upper Jaramillo catchments, respectively. Moreover, when adding the variance explained by the third PC, 12.17% (La Jara) and 14.95% (Upper Jaramillo), the cumulative variability increases to 92.53% in the La Jara catchment and 90.13% in the Upper Jaramillo catchment. Furthermore, while PC1 satisfies the aforementioned "rule of

1” in the History Grove catchment, explaining 76.95% of its stream chemistry variance, PC2 seems to be significant (16.56%), accounting for 93.51% of the overall variability.

4.2 End-members selection and projections

Once the number of principal components was established, equation [2] was used to project the standardized concentrations of the stream and potential end-members water samples onto a new dimensional subspace, i.e. U-space (Figures 3, 4 and 5). Moreover, the dimensionality of the U-space conditions the number of potential end-members that explain streamflow generation in each catchment, i.e. two- and three-dimensional U-spaces require three and four end-members, respectively.

The orthogonal projections of end-members and stream water chemistry in the two-dimensional U-spaces of the La Jara (Figure 3a) and Upper Jaramillo (Figure 4a) catchments show that snowmelt, rainfall and shallow soil water are the end-members that best bound the streamflow samples for these catchments. Additionally, History Grove spring (HGS) may also be an important water contributor in the La Jara catchment (Figure 3a). Even though HGS is not physically connected to Upper Jaramillo and La Jara catchments, a groundwater reservoir similar to History Grove spring groundwater may contribute to streamflow in these watersheds. Moreover, the U-space of the History Grove catchment (Figure 5a) suggests that snowmelt, rainfall and HGS are the most likely end-members to best describe the surface water chemical composition.

Furthermore, when assessing the U-spaces of three dimensions it is observed that snowmelt, rainfall, shallow soil water and HGS are the end-members that likely contribute to the streams in the three catchments (Figures 3b, 4b and 5b). Furthermore,

HGS and shallow soil water are common end-members among the catchments, these water sources are hereinafter referred to as ground water (GW) and soil water (SW).

Projected concentrations of streamflow and end-members were calculated using equation [3]. Additionally, the Euclidean distances between the projected and the observed concentrations were calculated for each end-member (Table 3). It is observed that the differences between the original and the projected chemical spaces for snowmelt and rainfall are large in all the catchments for all major cations and anions, except for water isotopes. Since these waters are very dilute, any difference would represent a significant percentage of change between the projected and observed concentrations (Liu et al., 2004). Liu et al., 2004, and Christophersen and Hooper, 1992 observed similar differences in Euclidean distances. Moreover, the relative low distances observed for the soil water and groundwater end-members demonstrate their significance to the EMMA analysis, and, consequently their relevance as headwaters in the system. Nevertheless, relatively greater percentages are observed for K^+ , TIC and Ca^{2+} .

Finally, although it is reasonable to assume that the higher the dimensions of the mixing U-space are, the estimation of source waters that contribute to surface flows would be more accurate. It is also important, however, to assess whether the identified potential end-members, i.e. three or four end-members for a two or three-dimensional U-space respectively, are relevant to explain streamflow generation in each case. The following section provides a general assessment of this conundrum.

5. DISCUSSION

An EMMA analysis that includes PCA utilizes all possible conservative tracers and, theoretically, it would be possible to identify all potential source waters that contribute to the chemical composition of the surface water. Nevertheless, the complexity of the system and climate may condition the degree of detail of the mixing model and the way the results are interpreted. The following section provides insights of how varying the dimensions of a mixing space, e.g. two- or three-dimensions, one can better discern whether the identified end-members provide statistical significance to explain the generation of streamflow in the La Jara, Upper Jaramillo, and History Grove catchments. Furthermore, the juxtaposition of these three catchments around Redondo peak will further our EMMA interpretation identifying the hydrologic processes that prevail in each catchment, as well as highlighting fundamental similarities and differences in their hydrologic regimes.

5.1 Analysis of U-mixing spaces

In a PCA the first eigenvector, i.e. principal component (PC), typically explains most of the variability of the original data set. As the subsequent PCs are added up the overall explained data variance increases—for each PC added to the analysis, the mixing model requires an additional end-member. Our results show that either two or three principal components are enough to explain at least 75% of the variance of the solute concentrations in the three catchments. The system's hydrology, geology and climate conditions, however, may condition the number of end-member that would likely contribute to the surface water (Christophersen and Hooper, 1992), thus one must judge

the number of components to retain based on the system's properties, and whether additional end-members are justified (Doctor et al., 2006).

The two principal component mixing space (2-D U-mixing-space) for the Upper Jaramillo catchment (Figure 4a) shows that the possible end-members are snowmelt, rainfall and soil water. Moreover, the 3-D U-mixing space (Figure 4b) shows groundwater as the fourth end-member. It is important to point out that most of the stream water samples plot close to the groundwater end-member. This suggests that these waters have similar chemical compositions and that groundwater contributions may be high relative to the other end-members. As such, when calculating the contributions of each end-member of the three principal component mixing model the overall contribution of the groundwater source is approximately 67% of the total discharge (Figure 6b).

Furthermore, factor analysis of principal components provides further evidence of the importance of groundwater end-member in Upper Jaramillo streams. This analysis shows correlations between the variables (i.e., solutes) and the eigenvector (i.e. principal components) extracted from PCA (Jolliffe, 2002). The factor analysis of the Upper Jaramillo catchment shows that the first two principal components explain the concentrations of TIC, K^+ , Mg^{2+} , $\delta^{18}O$ and δD , whereas the third principal component is correlated with the aqueous silica concentrations (Si) (Figure 7b). Si is one of the main products of mineral weathering and it is usually related to shallow subsurface flow and/or groundwater contributions (Olshansky et al., 2018; White et al., 2019). These results suggest that groundwater is the most important water source of the Upper Jaramillo catchment (Zapata-Rios et al., 2016). While the 2-D U-mixing space overlooks its

contributions, principal component three seems to strengthen our EMMA results highlighting the relevance of groundwater to the catchment's water regime.

The end-member analysis of the La Jara catchment, on the other hand, shows a slightly different pattern that was not captured in the Upper Jaramillo mixing diagrams. The two- principal component U-mixing space (Figure 3a) suggests that the end-members are snowmelt, rainfall, and groundwater. However, it is also observed that another subset of end-members (i.e. soil water, snowmelt, and rainfall) also cluster most of the surface water data points. Though one can argue that the fact that the data cloud plots closer to the groundwater end-member, soil water contributions may not be relevant. Nonetheless, snowmelt and rainfall end-members are also relatively distant from the data points, and yet it has been observed that their contributions are relevant in the Upper Jaramillo catchment. Moreover, assuming that four end-members likely generate streamflow in the La Jara catchment, it would be difficult to calculate their contributions in a two-dimensional mixing-space—these estimations may overlap leading to unreliable results. On the contrary, the three-dimensional mixing diagram (Figure 3b) reaffirms snowfall, rainfall, soil water, and groundwater as the most plausible end-members, thereby allowing better estimations of their contributions (Figure 6a). Moreover, factor analysis strengthens the argument that the La Jara's EMMA analysis requires three principal components to assess streamflow—principal component three is responsible for explaining the variability of Si concentration in the stream which again suggests groundwater contributions (Figure 7a).

Finally, the U-mixing space of two principal components for the History Grove catchment shows that the potential end-members are rainfall, snowmelt, and groundwater

(Figure 5a). While the 3-D U-mixing diagram (Figure 5b) includes soil water as an end-member, it also shows that all the stream water samples plot far from this water source and, more importantly, they cluster around the three end-members identified in the 2-D U-mixing space (Figure 5a). Additionally, factor analysis shows that TIC, K^+ , Mg^{2+} , $\delta^{18}O$ and δD concentrations are correlated with the first principal component, and principal component two explains Si concentrations (Figure 7c). Furthermore, similar to what was found in the Upper Jaramillo and La Jara catchments, the estimations of end-member contributions (Figure 6c) show that the contributions of groundwater are significantly higher than the other end-members. Thus, three end-members (two principal components) are enough to explain surface water discharge in the History Grove catchment.

The proposed EMMA analysis shows that by increasing the dimensions of the U-mixing space in each catchment, we were able to justify the number of end-members that contribute to surface flow in the headwaters around Redondo Peak. Moreover, even though the three catchments rely on the same end-members to maintain streamflow, each of these source water contributions vary significantly within and among these three watersheds. The following section provides some generalization of the hydrology in each catchment based on our PCA and EMMA results.

5.2 End-members contributions and streamflow generation: Hydrologic responses

The end-member mixing analysis results shows that snowmelt, rainfall and groundwater are important sources of streamflow in the three headwater catchments around Redondo peak. Soil water contributions, however, seems to be relevant only in the La Jara and Upper Jaramillo catchments, and are neglected in the History Grove

catchment. Furthermore, the estimated contributions of these end-members vary among the three catchments (Figures 6) suggesting that these headwaters have different hydrologic regimes that might be influenced by the catchment's physical features—e.g., aspect and subsurface structure—and/or climate variability.

The fraction of total discharge of each sampling event expresses the relative contributions of each end-member. Groundwater is the most salient source water among the three catchments (Figures 6). Most of its inputs to the streamflow happened primarily during the melt season—representing approximately 80%, 60% and 65% of total discharge for the Upper Jaramillo, La Jara and History Grove catchments respectively. Similarly, previous investigations at the site have shown that deep groundwater and subsurface lateral flow are the primary sources of water in the JRB-CZO system (Liu et al., 2008a; Zapata-Ríos et al. 2015; McIntosh et al., 2017; White et.al, 2019). The geology around Redondo peak is highly heterogenous and may influence the chemistry of the water flowing in the vadose zone and groundwater reservoirs. Our results show that History Grove spring—or groundwater similar to this spring—is the most salient end-member in the three catchments. Even though spring waters may not be composed entirely of groundwater (Frisbee et al., 2013; White et.al., 2019), these waters may capture the chemical signature of the stored groundwater in the underlying and surrounding geologic formations. The waters that converge to the outlet of the History Grove spring flow primarily through the Bandelier Tuff rock type which is the most common rock type in the three headwater catchments (Figure 1). The recent drilling campaign that took place in the JRB-CZO allowed us to directly characterize the groundwater at different depths (Figure 1). White et al. (2019) argued that deep

groundwater from the east side of the zero order basin (ZOB) at the JRB-CZO—located in the welded tuff (Figure 1)—is the most representative groundwater that contributes to the La Jara stream. Thus, it would be fair to assume that groundwater contributions to the creeks around Redondo peak come, for the most part, from this welded tuff rock type.

Furthermore, the variability of groundwater contributions among the three catchments may indicate differences in subsurface flow paths and water transient times (WTT). Lower vegetation water consumption and evaporation rates in the north-facing catchment, i.e., Upper Jaramillo, indicate higher water availability; consequently, larger mineral weathering rates and longer water transient times prevail in this catchment (Zapata-Ríos et al., 2016). These conditions allow most of the water inputs to reach the deep groundwater, thereby expecting greater groundwater contributions to the Upper Jaramillo creek (Figure 6b), which in turn influences its chemical signature—as evidenced in the 3-D U-mixing space (Figure 5b).

Conversely, the south-east facing catchments (La Jara and History Grove) are generally more water-limited (McIntosh et al., 2017; Zapata-Ríos et al., 2016). Even though groundwater contributions are high relative to the other end-members (Figures 6a and 6c), higher vaporization rates and biomass productivity, due to high energy inputs, may affect water partitioning processes in these catchments (Zapata-Ríos et al., 2016). Generally, peak flow in the La Jara and History Grove creeks occur earlier than in the north facing catchment (Upper Jaramillo) (Zapata-Ríos et al., 2016) suggesting that water transient times in the south-east facing catchments may be shorter and/or water routing through the subsurface is more complex (White et al., 2019). Recent studies have argued that deep groundwater is the main source of La Jara creek (McIntosh et al., 2017; White

et al., 2019), whereas shallow groundwater (e.g., perched aquifers) represent small volumetric contributions to streamflow (White et al., 2019). Nevertheless, relatively quick mineral dissolution and cation exchange within the subsurface in the JRB-CZO allow fresh water—e.g., snowmelt and rainfall—to accumulate solutes rapidly maintaining these concentrations high in the shallow groundwater that are later observed in the surface waters (Olshansky et al., 2018). During high water flow periods—i.e., snowmelt season—the water table of the deep groundwater rises and mixes with soil water and perched aquifers which increases surface water discharge (McIntosh et al., 2017; Olshansky et al., 2018; White et al., 2019). In dry seasons, however, deep groundwater seems to be disconnected from the stream channel, thus perched aquifers and shallow subsurface flow sustain streamflow in La Jara creek (McIntosh et al., 2017; White et al., 2019). Even though our EMMA analysis does not include water samples from the perched aquifer and the deep groundwater, we observe that the seasonal variability of the selected end-members mimic the hypothesized mechanisms that govern the subsurface water regimens in the La Jara catchment. During the snowmelt seasons we observed high groundwater contributions—i.e., deep groundwater is the most salient end-member as posited by McIntosh et al., (2017)—while during post-snowmelt and summer seasons soil water, snowmelt and rain fall contributions intensify (Figure 6a). The latter observations would not necessarily indicate direct inputs of these end-members to the stream. The water that percolates into the vadose zone takes different paths that may influence its chemistry. Olshansky et al. (2018) postulate that groundwater recharge at the ZOB in the JRB-CZO occurs via matrix and fracture flow. That is, the water flowing through the soil and the regolith matrix may take longer to reach the groundwater,

thereby reaching high solute concentrations—similar to soil pore-water concentrations. Conversely, water flowing through fractures moves faster through the vadose zone, reaction times are shorter, and thus relatively more diluted waters reach the water table—e.g. isotopic composition of snow and rainfall may be preserved. These chemically distinct waters mix in the shallow groundwater and are later transported to the surface water and/or mix with the deep groundwater. Thus, a possible explanation of the relatively high contributions of soil water, snowmelt and rainfall end-members in our EMMA is that these source waters mix in the perched aquifer, and the water that is later transported from this reservoir to La Jara creek flows primarily through the fractured regolith—high flow rate and short residence time—thereby preserving the chemical signature of soil water, snow, and rainfall in the stream. Similar trends but in less magnitude are observed in the Upper Jaramillo catchment where deep groundwater dominates surface flows.

In the History Grove catchment, however, our mixing model found that soil water contributions are negligible. The most salient end-member in this creek was groundwater—presumable deep groundwater as observed in the Upper Jaramillo and La Jara catchments. Furthermore, groundwater contributions the History Grove catchment follow similar patterns as that of the other two catchments, i.e., high pulses of groundwater into the stream are observed during wet periods, and these inputs gradually decrease as dry conditions prevail in the system—snow and rainfall contributions, on the other hand, increase (Figure 6c). The latter observation, again, can be interpreted as water predominantly flowing through the fractured welded tuff recharging the deep groundwater and/or feeding the surface water streamflow. Moreover, because this

fractured Bandelier Tuff rock type formation is dominant in the History Grove catchment (Figure 1), the volume of water moving through the soil and regolith matrixes in different geologic formations, and that captures the soil water signatures may not be significant, as shown in the three-dimensional mixing diagram (Figure 5b).

Finally, the calculated fractions of each end-members show significant differences when comparing the water years (WY) 2011 and 2012 in the three catchments. Water year 2012 was considerably wetter than 2011. The maximum snow water equivalent (SWE) in WY 2012 was 11 cm, whereas WY 2011 maximum SWE was 5.1 cm—total precipitation during summer monsoon was approximately 275 mm in both water years. Larger snow packs prevent soils from freezing which facilitates melted water percolating into the subsurface (Brooks et al., 1999), whereas smaller snow accumulations, may cause soils to freeze reducing soil infiltration capacity (Molotoch et al., 2009). Our EMMA results show that during the snowmelt season groundwater contributions dominate flow generation in the three headwaters around the dome, despite snow accumulation differences in water years 2011 and 2012. Even though snowmelt infiltration into the vadose zone may be smaller in WY 2011 than WY 2012 due to soil frost conditions, the infiltrated water creates a pressure gradient that stimulates the propagation of the deep groundwater to surface flows during melting periods in the three catchments (Figure 6) (McIntosh et al., 2017; White et al., 2019). Moreover, snowmelt, rainfall and soil water contributions during dry periods were greater in WY 2011 than in WY 2012 (Figures 6). The relative low volumes that infiltrated into the subsurface in WY 2011 feed both the perched aquifer and deep groundwater; nevertheless, as the snow pack thaws the percolated snowmelt and the late spring and summer precipitation volumes may not be

enough to keep deep groundwater propagations to the streams, i.e., groundwater contributions decrease significantly (Figures 6), thus shallow groundwater—whose chemistry has been assumed to be the mix of snowmelt, rainfall and soil water—is responsible to maintain flow in the creeks. Conversely, the predominantly wet conditions of WY 2012 allow enough of a hydraulic gradient in the subsurface even through drier periods (Figure 6)—deep groundwater is constantly pushed to the surface. It is important to point out that even though deep groundwater contributions after snowmelt seasons are significantly smaller in WY 2011 than WY 2012, our EMMA results show that this source water may not be entirely disconnected from the creeks.

The deep and shallow groundwaters from monitoring wells installed in the ZOB at the JRB-CZO provide further evidence of how these groundwater reservoirs interact with the surface waters of Redondo Peak (cf. McIntosh et al., 2017; Olshansky et al., 2018; White et al., 2019; Moravec et al., In Review). Future work should consider the groundwater data from the monitoring wells along with methodology presented in this study to look closer at the seasonal variability of end-members in the headwaters around Redondo Peak.

6. CONCLUSIONS

A multivariate end-member mixing analysis based on principal component analysis is an effective tool in watershed hydrology. In this study we focused on the dimensionality of the mixing spaces (U-space), i.e., the number of principal components retained, to justify the number of end-members that likely generate streamflow in each catchment. Deep groundwater dominates streamflow generation of the three headwater catchments in the JRB-CZO, as posited by McIntosh et al. (2017) and White et al. (2019). Moreover, shallow groundwater—whose chemistry has been assumed to be the mix of snowmelt, rainfall and soil water end-members—and subsurface lateral flow through the fractured tuff may actively support the generation of streamflow during dry periods in the three headwaters of the JRB-CZO.

Moreover, snowpack accumulation and changes in snow distribution and snowmelt rates affect hydrologic responses in these high elevation ecosystems. Semiarid forested catchments, such as the headwaters of the JRB-CZO, rely on precipitation inputs to recharge both the unsaturated and saturated zones. Climate variability alters precipitation patterns geographically and affect groundwater recharge rates, and consequently groundwater propagations to the surface waters.

The research that has been done at the JRB-CZO have sought to understand the deep and shallow groundwater flow paths and their interactions with the surface. The proposed methodology along with the deep and shallow groundwater sources and the well-known architecture of the subsurface at the JRB-CZO, may further our current of understanding of seasonal variability of end-member contributions around Redondo Peak.

7. FIGURES AND TABLES

Figure 1. Location of the Valles Caldera National Preserve in northern New Mexico. Redondo Peak, headwater catchments draining different aspects and springs locations around the dome.

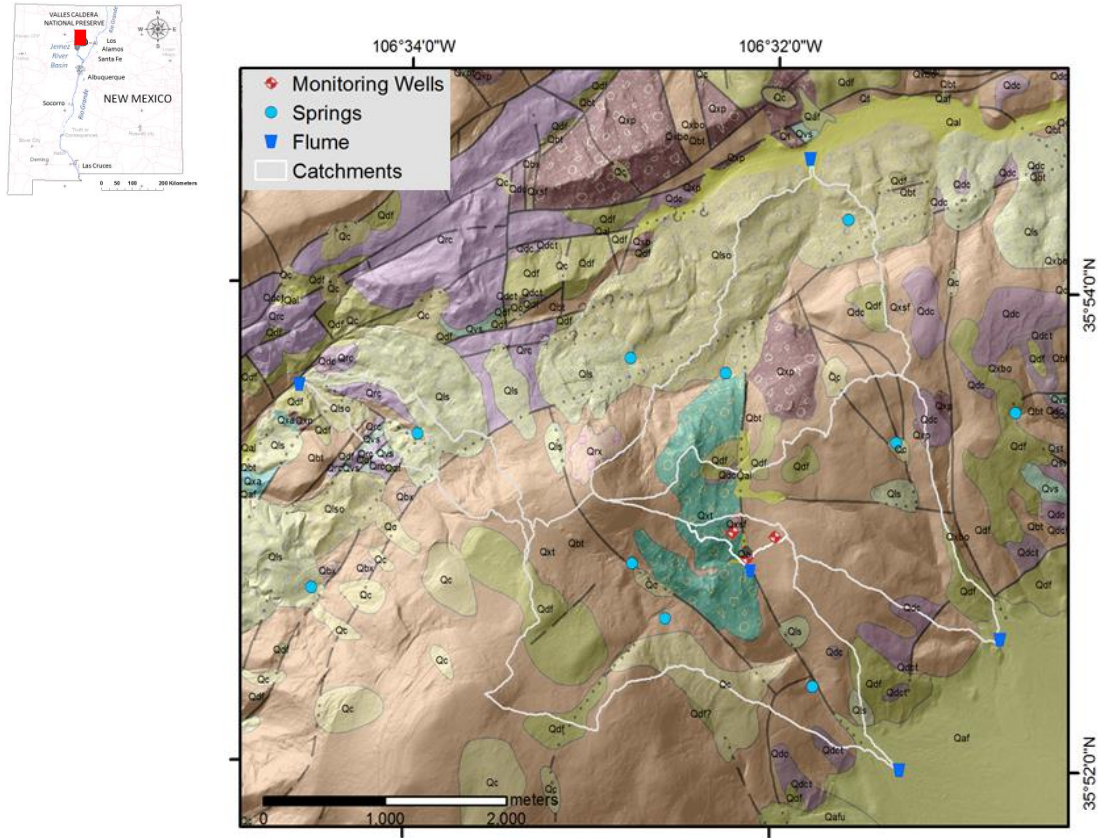


Figure 2. Conservative tracers evaluated by plotting medians of potential end-members along with solute concentrations of stream flow. (a) Shows an example of a bivariate plot with two tracers that are used in PCA, whereas (b) presents two tracers that cannot be utilized in PCA. A total of 55 mixing diagrams were evaluated for each catchment.

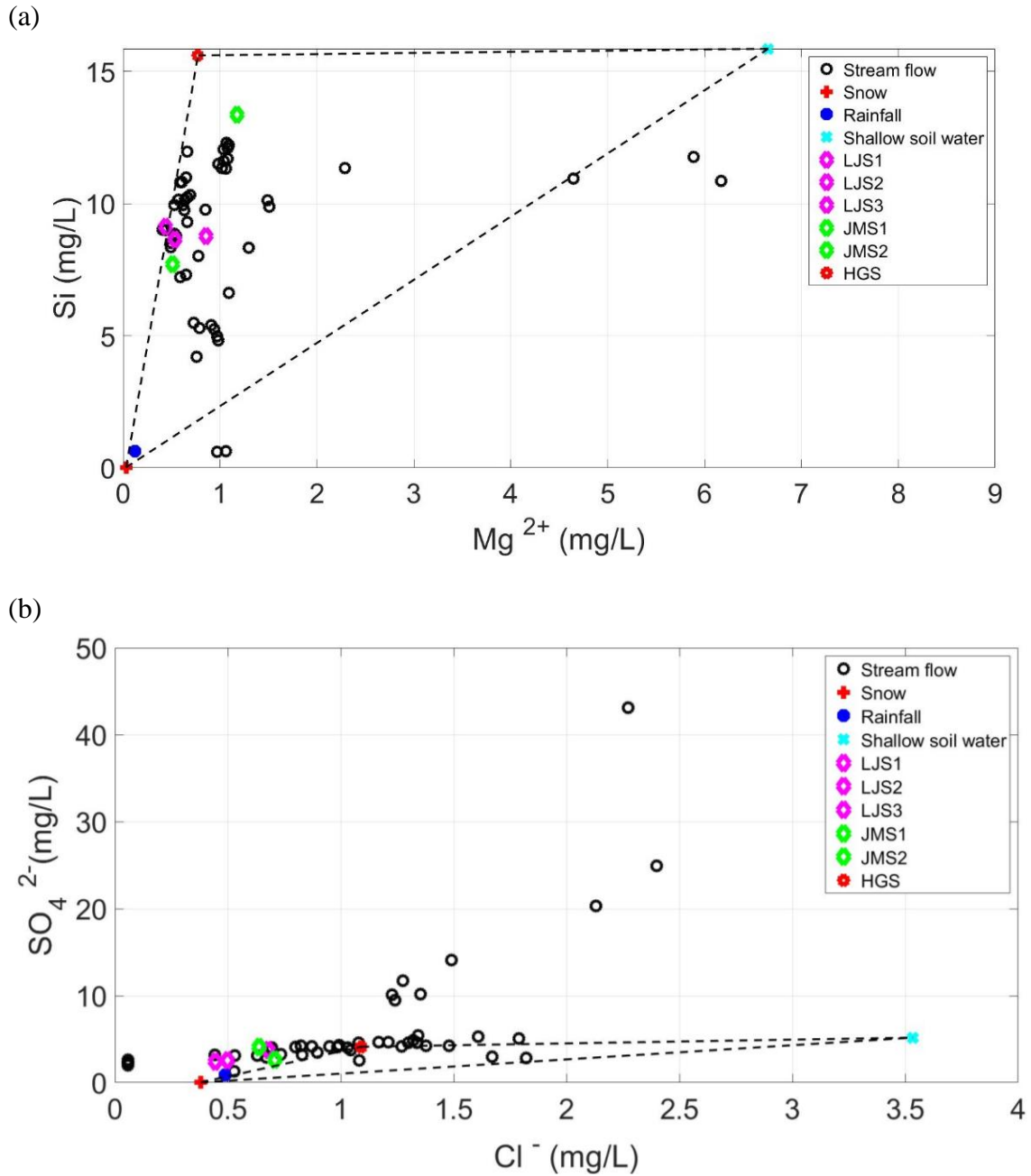


Figure 3. Orthogonal projection of end-members, onto (a) 2-D and (b) 3-D mixing U-spaces defined by stream water chemistry in La Jara catchment.

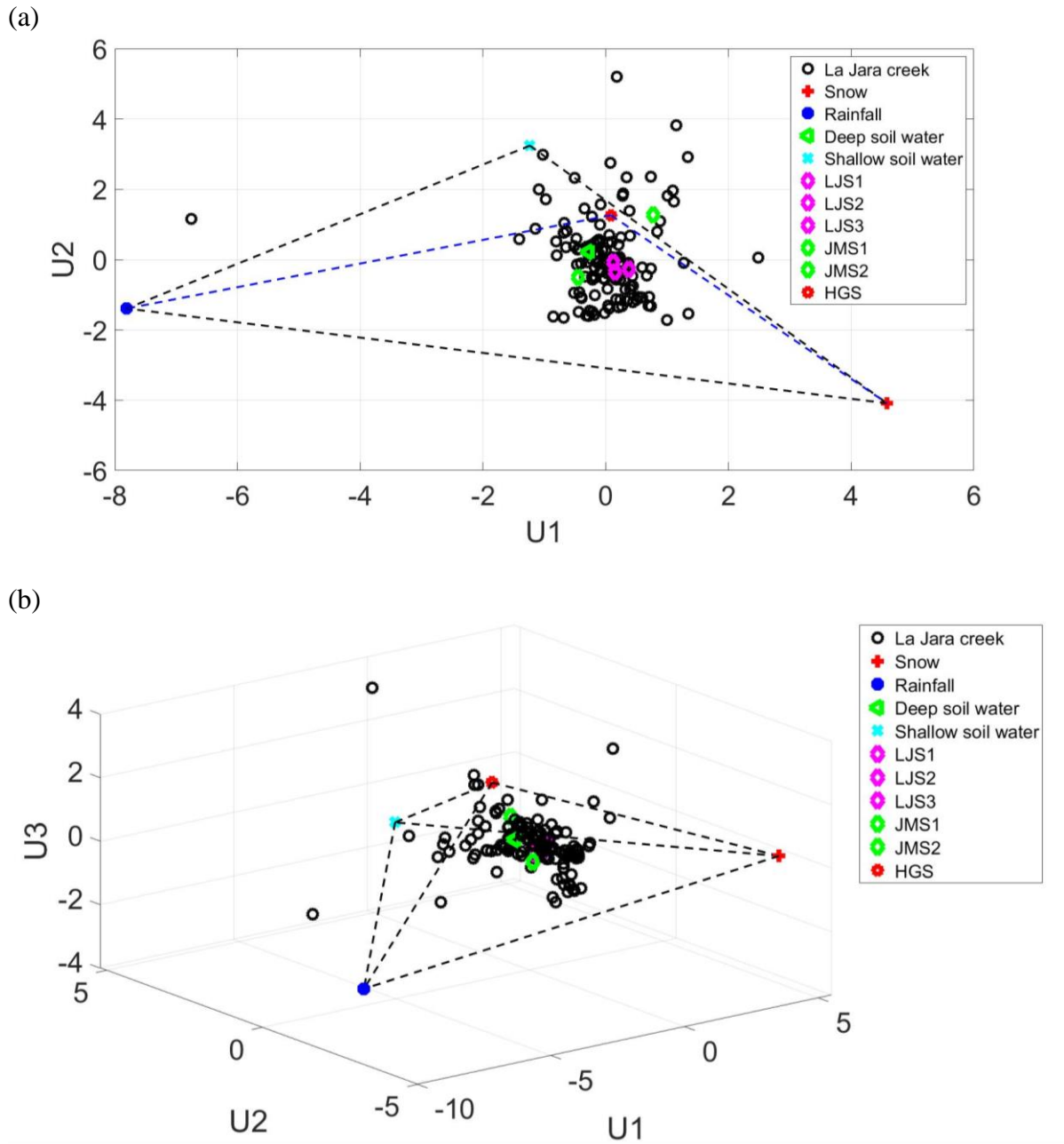


Figure 4. Orthogonal projection of end-members, onto (a) 2-D and (b) 3-D U spaces defined by stream water chemistry in Upper Jaramillo catchment.

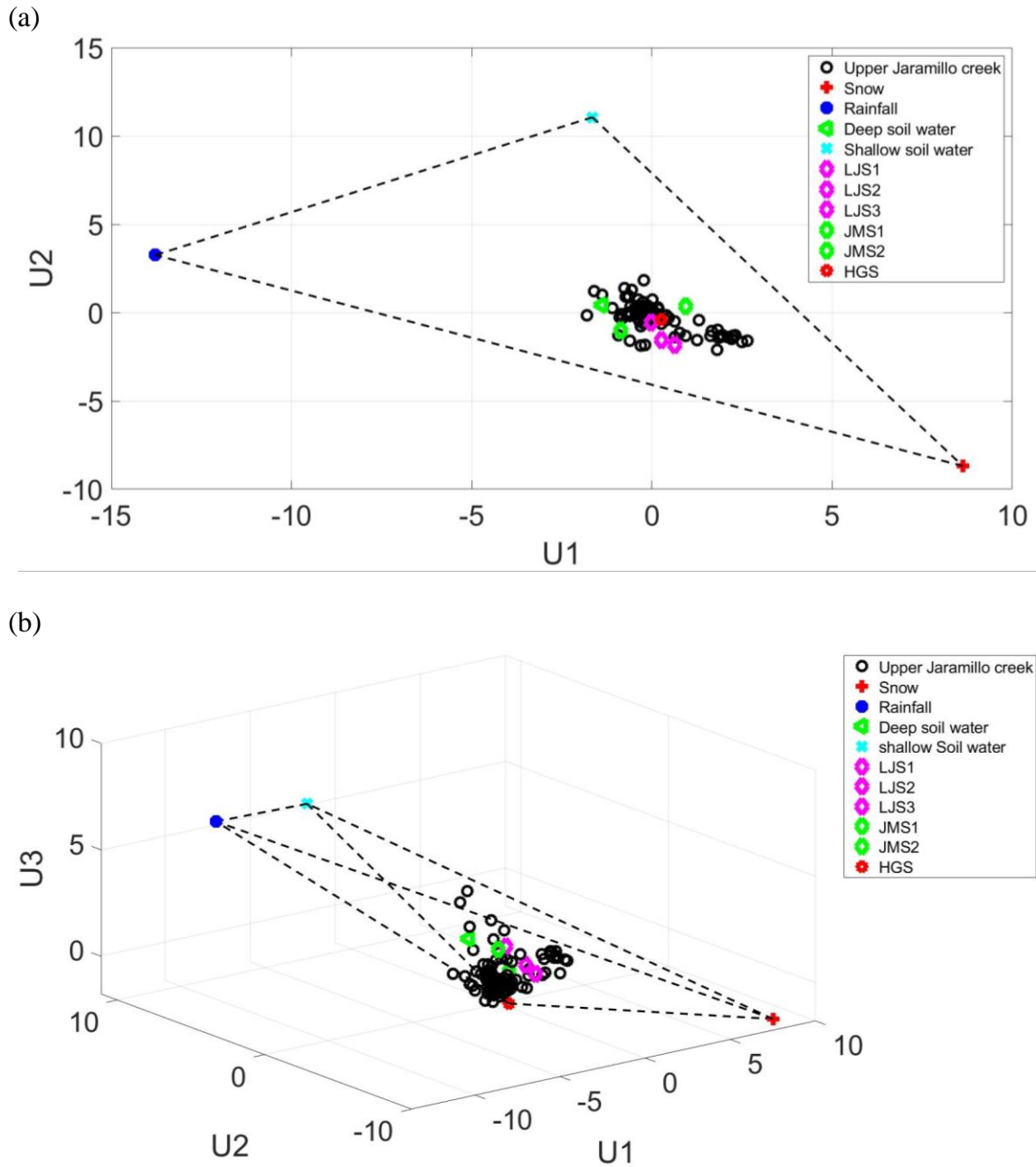


Figure 5. Orthogonal projection of end-members, onto (a) 2-D and (b) 3-D U spaces defined by stream water chemistry in History Grove catchment.

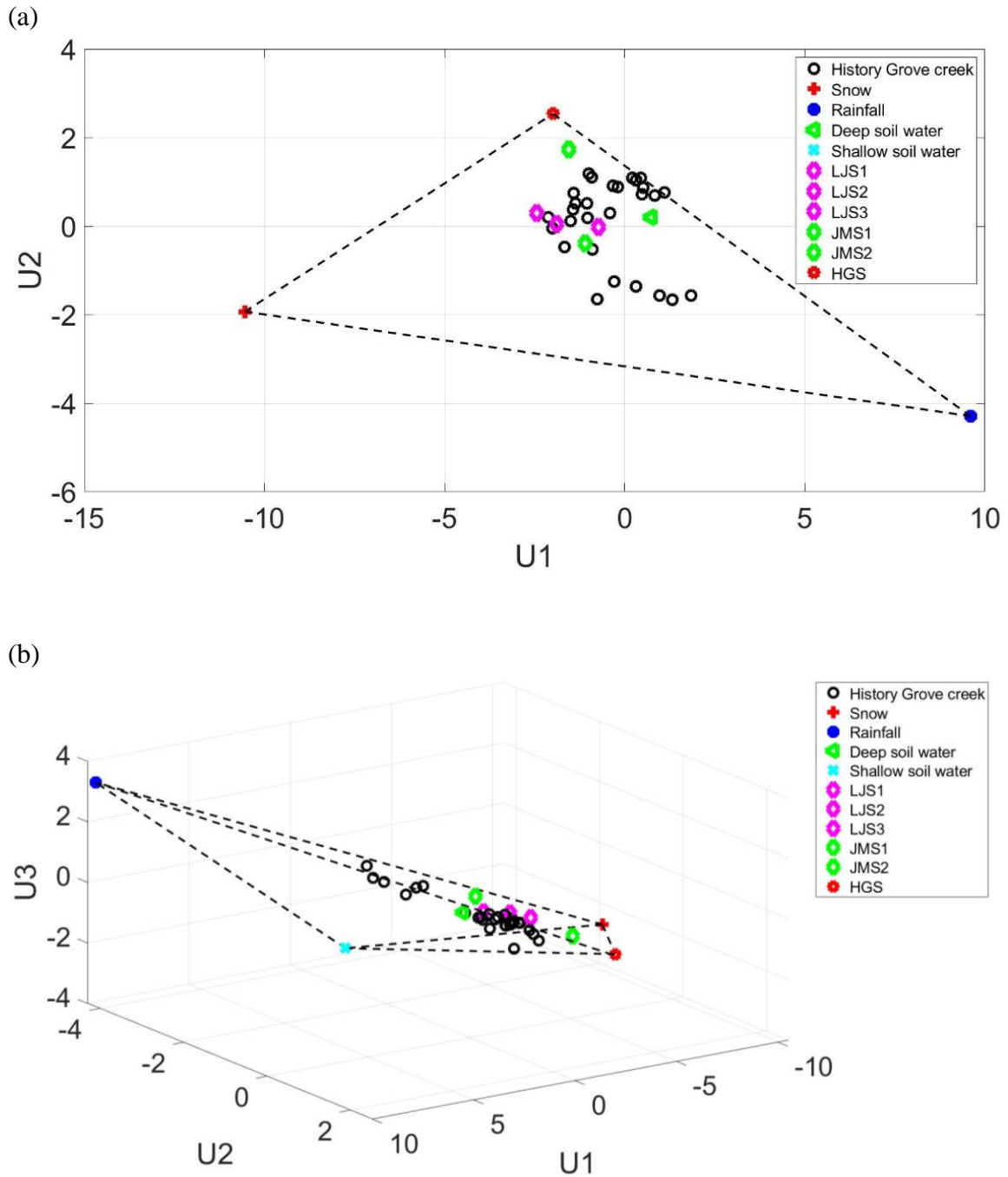


Figure 6. Calculated fractional contribution of selected end-members of the (a) La Jara, (b) Upper Jaramillo, and (c) History Grove creeks.

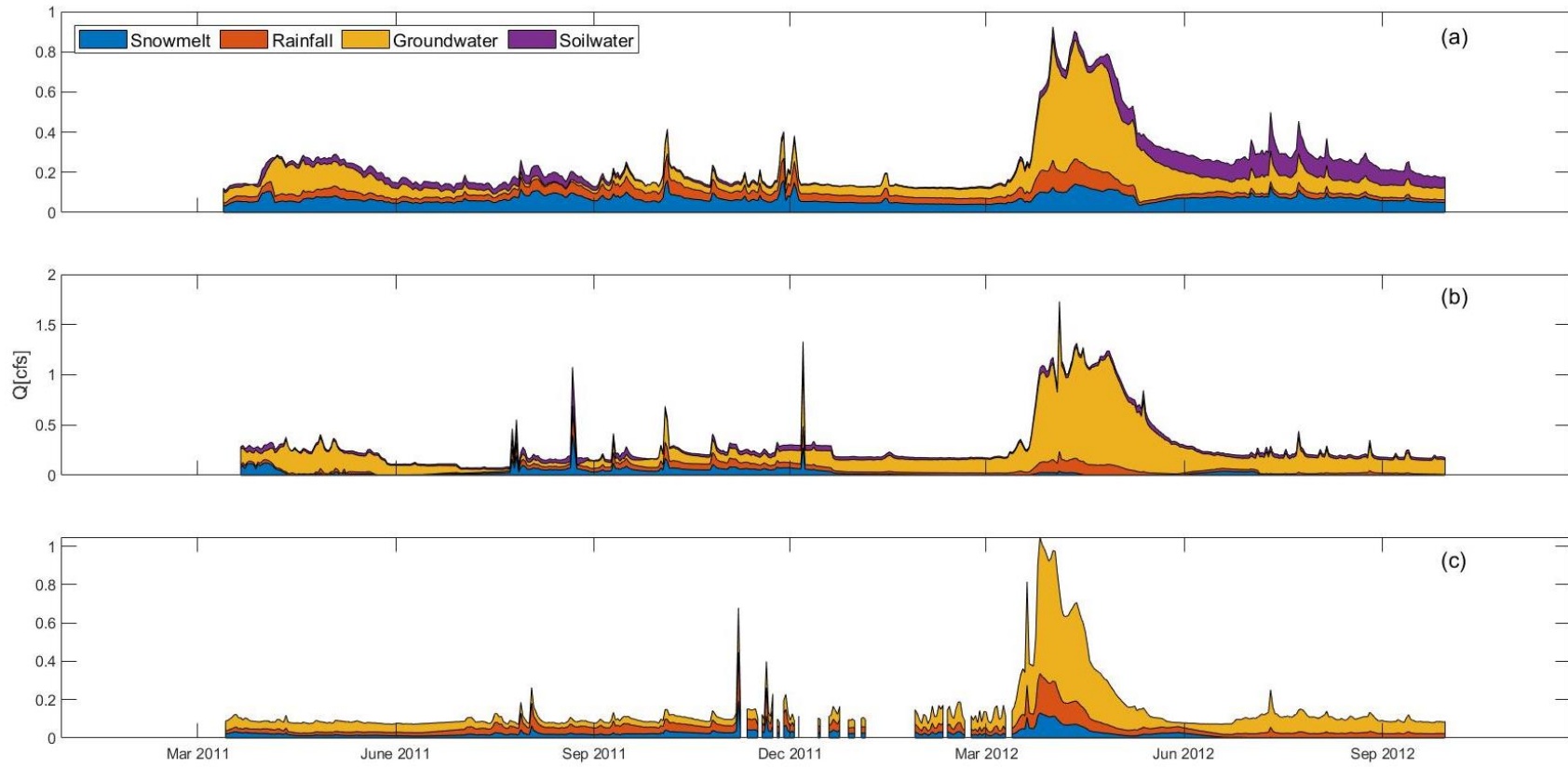
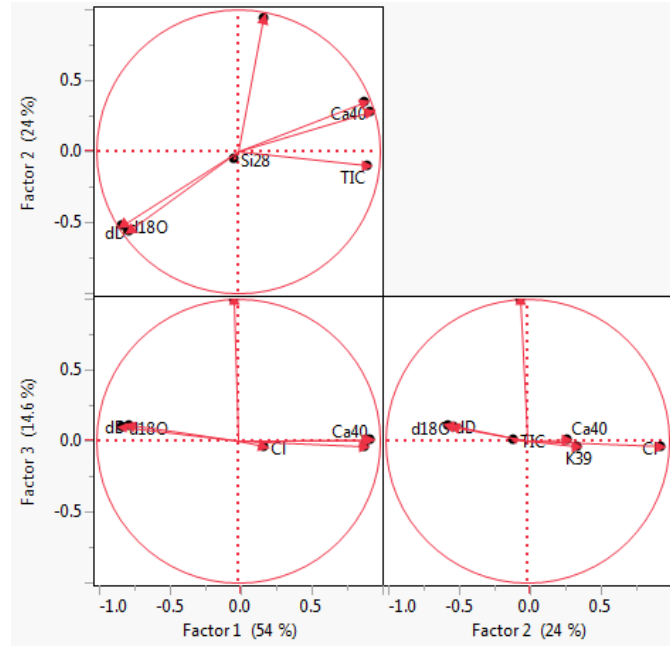
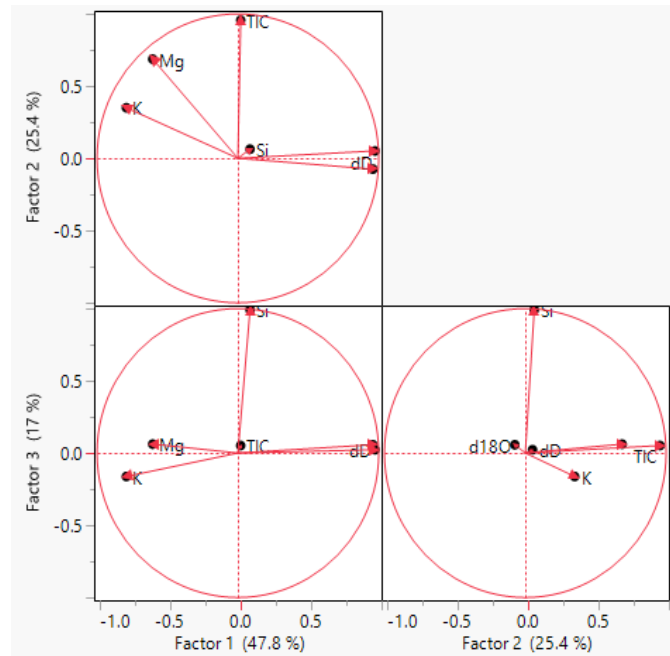


Figure 7. Factor Analysis of principal components retained for each mixing space in the La Jara (a), Upper Jaramillo (b), and History Grove (c) catchments.

(a)



(b)



(c)

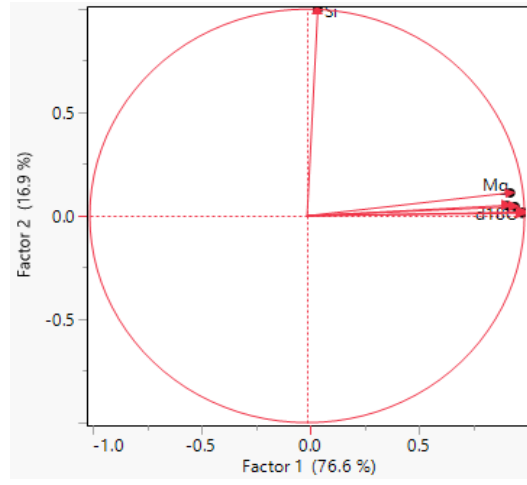


Table 1. Chemical composition of potential end-members (e.g. snow, rainfall, deep soil water, shallow soil water, La Jara spring 1 (LJS1), La Jara spring 2 (LJS2), La Jara spring (LJS3), Jaramillo spring 1 (JMS1), Jaramillo spring (JMS2), History Grove spring (HGS)). Median, and standard deviation in parenthesis.







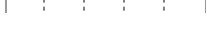
End-member	DIC (mg/L)	DOC (mg/L)	Cl ⁻ (mg/L)	SO ₄ ²⁻ (mg/L)	Na ⁺ (mg/L)	Mg ²⁺ (mg/L)	Si (mg/L)	K ⁺ (mg/L)	Ca ²⁺ (mg/L)	δD (‰)	δ ¹⁸ O (‰)	Tritium age (years)*
Snow	0.627 (0.728)	1.859 (2.145)	0.380 (0.470)	0.020	0.053 (0.173)	0.031 (0.455)	0.021 (0.380)	0.259 (0.388)	0.417 (0.475)	-125.511 (25.151)	-16.830 (2.961)	
Rainfall	2.621 (1.746)	3.869 (9.858)	0.487 (0.692)	0.890 (0.933)	0.118 (0.167)	0.123 (0.239)	0.642 (0.651)	0.508 (4.157)	1.352 (1.808)	-37.768 (26.401)	-6.215 (3.835)	
Deep soil water	5.140 (11.439)	18.708 (20.440)	1.406 (2.629)	6.649 (11.928)	3.610 (10.774)	1.016 (5.396)	9.888 (7.175)	1.833 (1.886)	10.223 (8.110)	-80.603 (11.411)	-11.390 (1.325)	
Shallow soil water	15.490 (20.628)	32.453 (109.592)	3.534 (4.405)	5.170 (6.489)	19.986 (30.943)	6.659 (7.550)	15.861 (7.033)	4.032 (17.464)	19.342 (35.119)	-54.937 (26.219)	-8.228 (3.147)	
LJS1	4.133 (0.714)	1.241 (0.353)	0.497 (0.246)	2.581 (1.981)	2.815 (0.384)	0.537 (0.137)	8.642 (3.926)	0.864 (0.504)	5.416 (2.642)	-88.407 (1.371)	-12.808 (0.175)	4.6 ± 1.1
LJS2	5.291 (1.760)	2.568 (4.626)	0.679 (0.662)	3.741 (3.879)	2.496 (0.595)	0.856 (0.450)	8.771 (5.031)	1.580 (1.069)	7.225 (4.609)	-84.583 (3.657)	-12.361 (0.524)	6.4 ± 1.3
LJS3	4.102 (0.489)	0.604 (1.993)	0.444 (0.635)	2.399 (0.321)	3.186 (0.427)	0.437 (0.140)	9.133 (4.148)	0.667 (0.401)	5.608 (1.293)	-90.389 (2.767)	-13.099 (0.388)	6.1 ± 1.4

JMS1	4.924 (1.254)	0.625 (1.917)	0.708 (0.173)	2.608 (1.285)	3.463 (0.285)	0.513 (0.050)	7.701 (2.650)	0.388 (0.186)	5.667 (0.845)	-83.102 (0.672)	-12.540 (0.050)	6.4 ± 1.4
JMS2	7.350 (0.575)	1.585 (8.405)	0.639 (0.119)	4.102 (2.490)	5.020 (0.473)	1.175 (0.119)	13.364 (5.456)	0.648 (0.437)	10.702 (2.730)	-88.811 (0.730)	-12.895 (0.028)	7.0 ± 1.3
HGS	4.037 (0.557)	1.181 (5.689)	1.091 (0.377)	4.120 (1.585)	2.449 (0.342)	0.774 (0.113)	15.606 (6.439)	0.366 (0.370)	4.898 (2.666)	-89.744 (1.312)	-12.871 (0.177)	5.1 ± 1.3







* Tritium ages obtained from Zapata at.al., 2015.

Table 2. Cumulative percentage of the eigenvalues from each eigenvector for each catchment.

La Jara

Number	Eigenvalue	Percent		Cum Percent
1	4.5836	65.479		65.479
2	1.0418	14.883		80.362
3	0.8515	12.165		92.527
4	0.2993	4.275		96.802
5	0.1365	1.950		98.752
6	0.0652	0.932		99.683
7	0.0222	0.317		100.000

Upper Jaramillo

Number	Eigenvalue	Percent		Cum Percent
1	3.1765	52.942		52.942
2	1.3345	22.242		75.184
3	0.8967	14.945		90.129
4	0.3086	5.143		95.272
5	0.2485	4.142		99.414
6	0.0351	0.586		100.000

History Grove







Number	Eigenvalue	Percent		Cum Percent
1	4.6168	76.946		76.946
2	0.9937	16.561		93.507
3	0.2882	4.803		98.311
4	0.0617	1.028		99.339
5	0.0364	0.607		99.946
6	0.0032	0.054		100.000

Table 3. Calculated Euclidean distances expressed in percentages for each conservative tracer, a) La Jara, b) Upper Jaramillo, and c) History Grove

a)

End-member	DIC	Cl⁻	Si	K⁺	Ca²⁺	δ¹⁸O	δD
Snow	-1246.29	-1995.77	12859.21	-2109.38	-7156.91	14.05	20.16
Rainfall	305.58	1815.35	-513.58	1387.22	2854.45	-51.18	-76.41
Shallow soil water	69.69	231.04	-17.03	133.14	122.92	-35.13	-40.69
History Grove spring	-10.70	-77.97	2.21	-282.31	-81.81	2.95	3.29

b)

End-member	DIC	Mg²⁺	Si	K⁺	δ¹⁸O	δD
Snow	1721.77	-3869.95	-10237.13	-2248.85	9.26	8.69
Rainfall	-418.26	1245.85	255.12	982.74	-28.57	-21.23
Shallow soil water	-113.03	56.95	0.04	70.99	-25.91	-16.66
History Grove spring	38.37	-6.60	-3.57	-374.40	3.01	1.42

c)

End-member	DIC	Mg²⁺	Si	K⁺	δ¹⁸O	δD
Snow	3393.70	20114.66	-8412.49	3761.30	15.54	18.05
Rainfall	-1019.47	-6227.90	341.91	-2385.53	-55.53	-69.60
History Grove spring	100.52	91.24	-1.39	223.65	3.40	2.20

8. REFERENCES

- Barmuta, L., A. Watson, A. Clark, and J. Clapcott (2009), The importance of the headwater streams, *Water Lines Report Series, No 25*, Australian Government, National Water Commission.
- Brantley, S. L., M. B. Goldhaber, and K. V. Ragnarsdottir (2007), Crossing disciplines and scales to understand the Critical Zone, *Elements*, 3, 307 – 314.
- Brooks P.D. and M.W. Williams, (1999). Snowpack controls on nitrogen cycling and export in high elevation catchments, *Hydrological Processes*. 13:2177-2190.
- Broxton, P.D., P.A. Troch, and S.W. Lyon, (2009). One role of the aspect to quantify water transit times in small mountainous catchments, *Water Resources Research*, 45, doi:10.1029/2008WR007438.
- Casas, J. J., A. Larranaga, M. Menendez, J. Pozo, A. Basaguren, A. Martinez, J. Perez, J.M. Gonzalez, S. Molla, C. Casado, E. Descals, N. Roblas, J.A. Lopez, and J.L. Valenzuela (2013). Leaf litter decomposition of native and introduced tree species of contrasting quality in headwater streams: How does the regional setting matter?, *Science of the Total Environment*, 197-208.
- Chipera, S., F. Goff, C. J. Goff, and M. Fittipaldo, (2008). Zeolitization of intracaldera sediments and rhyolitic rocks in the 1.25 Ma lake of Valles Caldera, New Mexico, USA, *Journal of Volcanology and Geothermal Research*, 178, Issue 2, 317 – 330.
- Christophersen, N., & Hooper, R. P., (1992). Multivariate analysis of stream water chemical data: The use of principal components analysis for the end-member mixing problem. *Water Resources Research*, 28(1), 99-107.
- Chorover, J., P. A. Troch, C. Rasmussen, P. D. Brooks, J. D. Pelletier, D. D. Breshears, T. E. Huxman, S. A. Kurc, K. A. Lohse, J. C. McIntosh, T. Meixner, M. G. Schaap, M. E. Litvak, J. Pedrial, A. Harpold, and M. Durcik, (2011). How water, carbon, and energy drive Critical Zone evolution: The Jemez-Santa Catalina Critical Zone Observatory, *Vadose Zone Journal*, 10, 884 – 899.
- Correa, A., Windhorst, D., Tetzlaff, D., Crespo, P., Célleri, R., Feyen, J., & Breuer, L. (2017). Temporal dynamics in dominant runoff sources and flow paths in the Andean Páramo. *Water Resources Research*, 53(7), 5998-6017.
- Dwivedi, R., Meixner, T., McIntosh, J. C., Ferré, P. T., Eastoe, C. J., Niu, G. Y., ... & Chorover, J. (2019). Hydrologic functioning of the deep critical zone and contributions to streamflow in a high-elevation catchment: Testing of multiple conceptual models. *Hydrological processes*, 33(4), 476-494.
- Doctor, D.H., Alexander Jr, E.C., Petrič, M., Kogovšek, J., Urbanc, J., Lojen, S. and Stichler, W., (2006). Quantification of karst aquifer discharge components during storm events through

end-member mixing analysis using natural chemistry and stable isotopes as tracers. *Hydrogeology Journal*, 14(7), pp.1171-1191.

Fee, E.J., Hecky, R.E., Kasian, S.E.M. and Cruikshank, D.R., (1996). Effects of lake size, water clarity, and climatic variability on mixing depths in Canadian Shield lakes. *Limnology and Oceanography*, 41(5), pp.912-920.

Frisbee, M. D., Phillips, F. M., White, A. F., Campbell, A. R., & Liu, F., (2013). Effect of source integration on the geochemical fluxes from springs. *Applied geochemistry*, 28, 32-54.

Goff, F., J.N. Gardner, S.L. Reneau, and C.J. Goff, (2006). Geologic map of the Redondo Peak quadrangle, Sandoval County, New Mexico, *New Mexico Bureau of Geology and Mineral Resources, New Mexico Tech*.

Gustafson, J. R., P.D. Brooks, N.P. Molotch, and W.C. Veatch, (2010). Estimating snow sublimation using natural chemical and isotopic tracers across a gradient of solar radiation, *Water Resources Research*, 46, W12511.

Heidbuchel, I., P. A. Troch, and S. W. Lyon, (2013). Separating physical and meteorological controls of variable transit times in zero-order catchments, *Water Resources Research*, 49, 7644 – 7657.

Hinckley, E.L.S., Ebel, B.A., Barnes, R.T., Anderson, R.S., Williams, M.W. and Anderson, S.P., (2014). Aspect control of water movement on hillslopes near the rain–snow transition of the Colorado Front Range. *Hydrological Processes*, 28(1), pp.74-85.

Hooper, R.P., (2003). Diagnostic tools for mixing models of stream water chemistry, *Water Resources Research*, 39(3), 1055, doi:10.1029/2002WR001528.

Huckle, D., Characterizing U-series isotope signatures in soils and headwater streams in a complex volcanic terrain: Jemez River Critical Zone Observatory, Valles Caldera, NM, *University of Arizona*.

Jolliffe, I., (2002). *Principal component analysis*. John Wiley & Sons, Ltd.

Kaplan, L. A., T. L. Bott, J. K. Jackson, J. D. Newbold, and B. W. Sweeney, (2008), Protecting headwaters: The scientific basis for safeguarding stream and river ecosystems, *STROUD Water Research Center*.

Kurtz, A.C., F. Lugolobi, and G. Salvucci, (2011). Germanium-silicon as flow path tracer: Application to the Rio Icacos watershed, *Water Resources Research*, 47, doi:10.29/2010WR009853.

Laudon, H., J. Seibert, S. Kohler, and K. Bishop, (2004). Hydrological flow paths during snowmelt: Congruence between hydrometric measurements and oxygen 18 in meltwater, soil water, and runoff, *Water Resources Research*, 40, W03102, doi:10.1029/2003WR002455.

Leopold, L. B., M. G. Wolman, and J. P. Miller, (1964). *Fluvial processes in geomorphology*. W. H. Freeman and Company: San Francisco.

Lohse, K. A., and P. Matson, (2005). Consequences of nitrogen additions for soil losses from wet tropical forests. *Ecological Applications*, 15(5), 1629-1648.

Liu, F., R.C. Bales, M.H. Conklin, and M.E. Conrad, (2008a). Streamflow generation from snowmelt in semi-arid, seasonally snow-covered, forested catchments, Valles Caldera, New Mexico, *Water Resources Research*, 44, doi:10.1029/2007WR006728.

Liu, F., R. Parmenter, P.D. Brooks, M.H. Conklin, and R. Bales, (2008b). Seasonal and interannual variation of streamflow pathways and biogeochemical implications in semi-arid, forested catchments in Valles Caldera, New Mexico, *Ecohydrology*, 1, 239 - 252.

Liu, F., Williams, M. W., & Caine, N., (2004). Source waters and flow paths in an alpine catchment, Colorado Front Range, United States. *Water Resources Research*, 40(9).

Lyon, S.W., P.A. Troch, P.D. Broxton, N.P. Molotch, and P.D. Brooks, (2008). Monitoring the timing snowmelt and initiation of streamflow using a distributed network of temperature/light sensors, *Ecohydrology*, 1, 215 – 224.

McGuire, K. J., McDonnell, J. J., Weiler, M., Kendall, C., McGlynn, B. L., Welker, J. M., & Seibert, J., (2005). The role of topography on catchment-scale water residence time. *Water Resources Research*, 41(5).

McIntosh, J. C., Schaumberg, C., Perdrial, J., Harpold, A., Vázquez-Ortega, A., Rasmussen, C., Vinson, D., Zapata-Rios, X., Brooks, P. D., Meixner, T, Pelletier, J., Derry, L., & Chorover, J., (2017). Geochemical evolution of the Critical Zone across variable time scales informs concentration-discharge relationships: Jemez River Basin Critical Zone Observatory. *Water Resources Research*, 53(5), 4169-4196.

Molotch, N.P., P.D. Brooks, S.P. Burns, M. Litvak, R. K. Monson, J. R. McConnell, and K. Musselman, (2009). Ecohydrological controls on snowmelt partitioning in mixed-conifer sub-alpine forests. *Ecohydrology*. 2:129-142. DOI: 10.1002/eco.48

Moravec, B. G., A. M. White, A., Root, R., Sanchez, R. A., Olshansky, Y., Paras, B. K., Carr, B., McIntosh, J., Pelletier, J. D., Rasmussen, C., Holbrook, W. S., and Chorover, J., (In Review). Resolving deep critical zone architecture in complex volcanic terrain.

Olshansky, Y., White, A. M., Moravec, B., McIntosh, J., & Chorover, J., (2018). Subsurface pore water contributions to stream concentration-discharge relations across a snowmelt hydrograph. *Frontiers in Earth Science*, 6, 181.

Page, R.M., G. Lischeid, J. Epting, and P. Huggenberger, (2012). Principal component analysis of time series for identifying indicator variables for riverine groundwater extraction management, *Journal of Hydrology*, 137 - 144.

Porter, C., (2012), Solute inputs to soil and stream waters in a seasonally snow-covered mountain catchment determined using Ge/Si, $^{87}\text{Sr}/^{86}\text{Sr}$ and major chemistry: Valles Caldera, New Mexico, *University of Arizona*.

Rademacher, L.K., J.F. Clark, D.W. Clow, and G.B. Hudson, (2005). Old groundwater influence on stream hydrochemistry and catchment response times in a small Sierra Nevada catchment: Segehen Creek, California, *Water Resources Research*, 41, doi:10.1029/2003WR002805.

Rasmussen, C., S.M. Meding, A. Vazquez, J. Chorover J., (2012). Domes, Ash and Dust – Controls on soil genesis in a montane catchment of the Valles Caldera, New Mexico. *Abstract EP42D-04 presented at 2012 Fall Meeting, AGU, San Francisco, Calif., 3-7 Dec (Talk)*.

Reyment, R. A., & Jvreskog, K. G., (1996). *Applied factor analysis in the natural sciences*. Cambridge University Press.

Vázquez-Ortega, A., J. Perdrial, A. Harpold, X. Zapata-Ríos, C. Rasmussen, J. McIntosh, M. Schaap, J.D. Pelletier, P. D. Brooks, M. K. Amistadi, and J. Chorover, (2015). Rare earth elements as reactive tracers of biogeochemical weathering in forested rhyolitic terrain, *Chemical Geology*, 391, 19 - 32.

White, A., Moravec, B., McIntosh, J., Olshansky, Y., Paras, B., Sanchez, R. A., Ferré, T. P. A., Meixner, T., and Chorover, J., (2019). Distinct stores and the routing of water in the deep critical zone of a snow-dominated volcanic catchment. *Hydrol. Earth Syst. Sci.*, 23, 4661–4683, <https://doi.org/10.5194/hess-23-4661-2019>.

Wilcox, B.P., B.D. Newman, D. Drandes, D.W. Davenport, and K. Reid, (1997). Runoff from a semiarid ponderosa pine hillslope in New Mexico, *Water Resources Research*, 33(10), 2301 – 2314.

Woff, J. A., K. A. Brunstad, and J. N. Gardner, (2011). Reconstruction of the most recent volcanic eruptions from the Valles Caldera, New Mexico, *Journal of Volcanology and Geothermal Research*, 199, 53 – 68.

Zapata, X., J. McIntosh, L. Rademacher, P.A. Troch, P.D. Brooks, C. Rasmussen, and J. Chorover, (2015). Climatic and landscape controls on water transit times and silicate mineral weathering in the critical zone, *Water Resources Research*.

Zapata-Rios, X., Brooks, P.D., Troch, P.A., McIntosh, J. and Guo, Q., (2016). Influence of terrain aspect on water partitioning, vegetation structure and vegetation greening in high-elevation catchments in northern New Mexico. *Ecohydrology*.